CELL STRUCTURE AND FUNCTION 43: 41–51 (2018)

A Missense Mutation in the *NSF* Gene Causes Abnormal Golgi Morphology in *Arabidopsis thaliana*

Sayuri Tanabashi[1], Keiko Shoda[2], Chieko Saito[1], Tomoaki Sakamoto[3], Tetsuya Kurata[3], Tomohiro Uemura[1], and Akihiko Nakano[1,4]*

[1]*Department of Biological Sciences, Graduate School of Science, The University of Tokyo, Hongo, Bunkyo-ku, Tokyo 113-0033, Japan,* [2]*Laboratory for Cell Function Dynamics, RIKEN Brain Science Institute, Hirosawa, Wako, Saitama 351-0198, Japan,* [3]*Graduate School of Biological Sciences, Nara Institute of Science and Technology, Takayama, Ikoma 630-0192, Japan,* [4]*Live Cell Super-Resolution Live Imaging Research Team, RIKEN Center for Advanced Photonics, Hirosawa, Wako, Saitama 351-0198, Japan*

ABSTRACT. **The Golgi apparatus is a key station of glycosylation and membrane traffic. It consists of stacked cisternae in most eukaryotes. However, the mechanisms how the Golgi stacks are formed and maintained are still obscure. The model plant *Arabidopsis thaliana* provides a nice system to observe Golgi structures by light microscopy, because the Golgi in *A. thaliana* is in the form of mini-stacks that are distributed throughout the cytoplasm. To obtain a clue to understand the molecular basis of Golgi morphology, we took a forward-genetic approach to isolate *A. thaliana* mutants that show abnormal structures of the Golgi under a confocal microscope. In the present report, we describe characterization of one of such mutants, named #46-3. The #46-3 mutant showed pleiotropic Golgi phenotypes. The Golgi size was in majority smaller than the wild type, but varied from very small ones, sometimes without clear association of *cis* and *trans* cisternae, to abnormally large ones under a confocal microscope. At the ultrastructual level by electron microscopy, queer-shaped large Golgi stacks were occasionally observed. By positional mapping, genome sequencing, and complementation and allelism tests, we linked the mutant phenotype to the missense mutation D374N in the *NSF* gene, encoding the *N*-ethylmaleimide-sensitive factor (NSF), a key component of membrane fusion. This residue is near the ATP-binding site of NSF, which is very well conserved in eukaryotes, suggesting that the biochemical function of NSF is important for maintaining the normal morphology of the Golgi.**

Key words: Golgi morphology, *N*-ethylmaleimide-sensitive factor (NSF), *Arabidopsis thaliana*

Introduction

The Golgi apparatus exists in all eukaryotic cells, which was first identified by Camillo Golgi. This organelle plays crucial roles in cargo sorting and processing such as glycosylation. The Golgi apparatus usually consists of flattened disk-shaped membrane called cisternae, each of which has distinct processing enzymes. These enzyme distributions show a conserved *cis*-to-*trans* polarity that reflects the order of oligosaccharide processing (Emr *et al.*, 2009), thus early acting enzymes dominate in *cis*-cisternae, whereas late-acting enzymes are concentrated in *trans*-cisternae (Nilsson *et al.*, 2009). The *cis*-side cisternae receive newly synthesized proteins from the endoplasmic reticulum (ER), which travel across the stack to the *trans*-side cisternae. Then they are sorted in the *trans*-Golgi network (TGN) and transported to their final destinations such as outside of the cell, the plasma membrane (PM) and lysosomes/vacuoles.

There has been a debate about how cargo proteins are transported in the Golgi. From mammalian-cell-based cell free assays, the vesicular transport model has been proposed, which assumes that the Golgi cisternae are stable static compartments and resident Golgi proteins are retained in the cisternae, while cargo proteins are conveyed by vesicles in the anterograde way (Rothman and Wieland, 1996). Another model, called the cisternal maturation model, considers that resident Golgi proteins move from later to earlier cisternae, thereby cisternae mature from *cis* to *trans*. Cargo can just stay in cisternae and eventually reach the *trans* side. This model was strongly supported by live imaging in the budding yeast *Saccharomyces cerevisiae* (Losev *et al.*, 2006; Matsuura-Tokita *et al.*, 2006), which clearly demonstrated that Golgi cisternae change

*To whom correspondence should be addressed: Akihiko Nakano, Live Cell Super-Resolution Live Imaging Research Team, RIKEN Center for Advanced Photonics, 2-1 Hirosawa, Wako, Saitama 351-0198, Japan.
Tel: +81–48–467–9547, Fax: +81–48–462–4679
E-mail: nakano@riken.jp

their properties from *cis* to *trans* over time. In either of the two models, vesicles are believed to play critical roles in transport. General mechanisms of vesicular transport should apply to these intra-Golgi events. Namely, vesicles are formed by the budding machinery, which comprises COPI (coat protein complex I) and the Arf GTPase, and are targeted to a particular cisterna by the fusion machinery, which involves tethers, Rab GTPases, NSF (*N*-ethylmaleimide-sensitive factor), SNAP (soluble NSF-attachment protein) and SNAREs (SNAP receptors). Indeed, the cisternal maturation in yeast is strictly controlled by COPI, again supporting the main frame of the model (Ishii *et al.*, 2016; Papanikou *et al.*, 2015). It should also be noticed, however, that tubular extensions and interconnections can also play roles in intra-Golgi transport (Glick and Luini, 2011; Glick and Nakano, 2009).

The Golgi consists of stacked cisternae in most eukaryotes. This principal structural feature of the Golgi is considered to reflect its function (Mollenhauer and Morré, 1991). However, there are marked variations among organisms in the morphological and organizational patterns of the Golgi. In the budding yeast *S. cerevisiae*, the Golgi does not form stacks and individual cisternae as transient structures are dispersed in the cytoplasm (Losev *et al.*, 2006; Matsuura-Tokita *et al.*, 2006; Preuss *et al.*, 1992). In mammalian cells by contrast, the Golgi forms a giant and complex ribbon-shaped structure, which is densely concentrated to the perinuclear centrosomal region. In flowering plants such as Arabidopsis and tobacco, the Golgi is in the form of mini-stacks of cisternae, which are individually functional units, being distributed throughout the cytoplasm and moving along actin filaments. In some green algae, the Golgi represents a large stack consisting of numerous cisternae (Noguchi, 1978; Staehelin and Kang, 2008). The Golgi apparatus in flowering plants is thus regarded as a nice model to study its morphology in detail by light microscopy.

To obtain a clue to understand the molecular mechanisms how the Golgi stacks are formed and maintained, we employed a forward-genetic approach combined with confocal microscopy-based visualization to isolate mutants from *A. thaliana* that show abnormal morphology of the Golgi. Among 30 mutant candidates we isolated, we describe in the present paper about the mutant #46-3, which shows aberrant structures of the stack. By positional mapping, genome sequencing, and complementation and allelism tests, we concluded that a D-to-N missense mutation in the *NSF* gene, encoding a key factor in membrane fusion, is the cause of the phenotype.

Materials and Methods

Plant materials and growth conditions

For wild-type plants of *A. thaliana*, ecotypes Colombia-0 (Col-0) and Landsberg *erecta* were used in this study. Seeds of the transgenic plant of *A. thaliana* (Col-0) expressing ERD2-GFP (Boevink *et al.*, 1998; Takeuchi *et al.*, 2000, 2002) (named A21) were mutagenized by treatment with 0.3% ethyl methanesulfonate (EMS) for 16 h. T-DNA insertion mutants, SALK_138721, SAIL_1155_C06 and SAIL_620_E12 were obtained from the Arabidopsis Biological Resource Center (Columbus, OH, USA). Mutants were backcrossed three times with the wild-type Col-0. Surviving seedlings were individually grown up and subjected to self-pollination to establish M2-generation lines. M2 seeds were sown on MS medium [1×MS salt, 1% sucrose, vitamin mix and 0.2% agar], vernalized in the dark at 4°C for 4 days, and grown at 23°C under continuous light. Selection media contained glufosinate ammonium salt (BASTA; final concentration 7.5 μg/ml) or kanamycin (50 μg/ml) for T-DNA insertion lines and hygromycin (25 μg/ml) for complementation lines.

Plasmid constructions

To isolate the *NSF* gene under its own promoter (*proNSF:NSF*), a genomic fragment was amplified by PCR using a primer set (5'-AACCAATTCAGTCGACTCGGAGAAAAGAGGGCAAGT-3' and 5'-AAGCTGGGTCTAGATAATGTTGTGCGAAGTGAGAGTC-3'). Gateway pENTR 1A dual selection vector (Thermo Fisher Scientific/Invitrogen, Waltham, MA, USA) was amplified by PCR using a primer set (5'-AACCAATTCAGTCGAC-3' and 5'-AAGCTGGGTCTAGATA-3'). After treatment of Gateway pENTR 1A with restriction enzymes *Sal*I and *Eco*RV, the genomic fragment was cloned into the vector pENTR 1A and recombined into pHGW (Karimi *et al.*, 2002) by LR Clonase II (Thermo Fisher Scientific/Invitrogen). Transformed lines were obtained with a floral dip procedure (Clough and Bent, 1998).

Isolation of the #46-3 mutant and genetic analysis

M2 ERD2-GFP seeds were grown for 16 days and observed under a confocal microscope. A homozygous mutant line named #46-3, showing abnormal morphology of the Golgi, was crossed with Landsberg *erecta* to generate a mapping population. *A. thaliana* ecotype-specific markers of simple sequence length polymorphisms (SSLPs) and cleaved amplified polymorphic sequences (CAPSs) (Konieczny and Ausubel, 1993; Bell and Ecker, 1994) were used for rough mapping on 20 individuals showing the abnormal Golgi phenotype. For genome-sequencing and SNPs calling, a modified method from Uchida *et al.* (2011) was used. SNPs calling was performed under Strand NGS software (Strand Life Sciences).

Confocal microscopy

For single-color imaging, transgenic plants were visualized under an Olympus IX81 fluorescence microscope equipped with a confocal laser-scanning unit (CSU10, Yokogawa Electronic, Tokyo, Japan) and images were acquired by a CCD camera ORCA-R2 (Hamamatsu Photonics, Hamamatsu, Japan). Dual-color imaging was carried out with a LSM780 confocal microscope (Zeiss, Jena, Germany). The central regions of petioles 16 days after germination were mounted with water on glass slides. Images were processed and analyzed with ImageJ 1.49i (National Institute of Health, Bethesda, MD, USA).

Electron microscopy

16-day-old petioles of seedlings (wild type and #46-3) were rapidly frozen in a high-pressure freezer (HPM010; Bal-Tec). Frozen samples were transferred to 2% osmium tetraoxide in anhydrous acetone that had been precooled with liquid nitrogen. Samples were maintained at –80°C for 7 days, at –20°C for 2 h, at 4°C for 2 h, and then at room temperature for 2 h. After several washes with anhydrous acetone, samples were embedded in Spurr's resin (Nisshin EM). Ultrathin sections (thickness 60–80 nm) were cut, stained with uranyl acetate and lead citrate, and observed under a transmission electron microscope (JEM-1010; JEOL).

Results

Isolation of a mutant with abnormality in the Golgi morphology

To isolate mutants that show abnormalities in the morphology of the Golgi apparatus, we decided to use the *A. thaliana* line that expresses ERD2-GFP driven by 35S promoter, a well-established *cis*-Golgi marker (Boevink *et al.*, 1998; Takeuchi *et al.*, 2000, 2002). The fluorescence of ERD2-GFP shows disk-like structures, which are dispersed through the cytoplasm. The parent line A21, expressing ERD2-GFP, was treated with ethyl methanesulfonate to induce mutations. After due processes, M2 lines were established and subjected to visual screening under a confocal microscope, Olympus IX81 equipped with a spinning-disk confocal unit CSU10. As the morphology of the Golgi appeared to vary in different tissues, we selected the third-leaf-petioles of 16-day-old seedlings, which reproducibly show large and bright Golgi structures. By manual examination of approximately 10,000 M2 lines, we selected 30 mutant candidates that showed altered shapes of the Golgi. The morphological phenotypes were of a wide variety; large, small, with tubules, large and bent, large aggregates, and so on. They were further subjected to crossing with the parent to determine dominant or recessive natures. The mutant line named #46-3, which is the subject of the present paper, displayed abnormalities in the size and shape of the Golgi and this phenotype turned out recessive to the wild type (see below). Otherwise, the #46-3 mutant did not show any discernible macroscopic phenotypes. The mutant plants grew normally and were fertile.

The abnormality of the Golgi morphology in #46-3 was the peculiarity of size and shape as shown in Fig. 1A. While the ERD-GFP fluorescence in the wild type showed mostly disk-like shapes in similar sizes, in the #46-3 mutant the shape looked irregular and the size varied from smaller to larger as compared to the wild type (Fig. 1A and B). To quantify the Golgi size, we measured the areas of fluorescent signals in 10 epidermal cells of petioles (expressed as pixels). The distribution of the Golgi size in the wild type and in #46-3 is shown as histograms in Fig. 1C. It clearly shows that the Golgi size of #46-3 is in majority smaller than the wild type. It should be noted that abnormally large Golgi was also occasionally seen in the #46-3 mutant (Fig. 1D).

Localization analysis of cis- and trans-Golgi in the #46-3 mutant

To further investigate the anomalies of the Golgi morphology, the arrangement of *cis* and *trans* cisternae in Golgi stacks was examined in the wild-type and #46-3 plants stably expressing ST-mRFP, a *trans*-Golgi marker (sialyl transferase from rat) (Boevink *et al.*, 1998; Ito *et al.*, 2012, 2017), in addition to ERD2-GFP. As shown in Fig. 2A, fluorescence signals of ERD2-GFP and ST-mRFP were mostly adjacent to each other. Sometimes the distance between the peaks of GFP and mRFP signals was markedly larger in the #46-3 mutant (Fig. 2B). GFP signals without associating mRFP signal were also occasionally observed in the #46-3 mutant (Fig. 2C).

Electron microscopic analysis of the Golgi structure in the #46-3 mutant

We next analyzed the Golgi morphology in the #46-3 mutant by transmission electron microscopy. The Golgi stacks in the wild-type Arabidopsis usually consist of around 5 cisternae as shown in Fig. 3A. Abnormally small Golgi structures, which were often seen in fluorescence, were not easy to identify in the leaf epidermal cells of #46-3, perhaps because they did not show typical stacks. Fig. 3B shows one example of electron micrograph showing two Golgi-like structures harboring 2–3 cisternae. We sometimes observed abnormal Golgi stacks consisting of increased numbers of cisternae in the #46-3 mutant. In the example shown in Fig. 3C, as many as 9 cisternae can be counted in what appeared to be a single Golgi stack. In another example (Fig. 3D), a Golgi stack bore an unusually large *trans*-most cisterna. To quantify the cisternal number per Golgi stack, we counted that in the epidermal cells of petioles. The distribution of the cisternal number in the

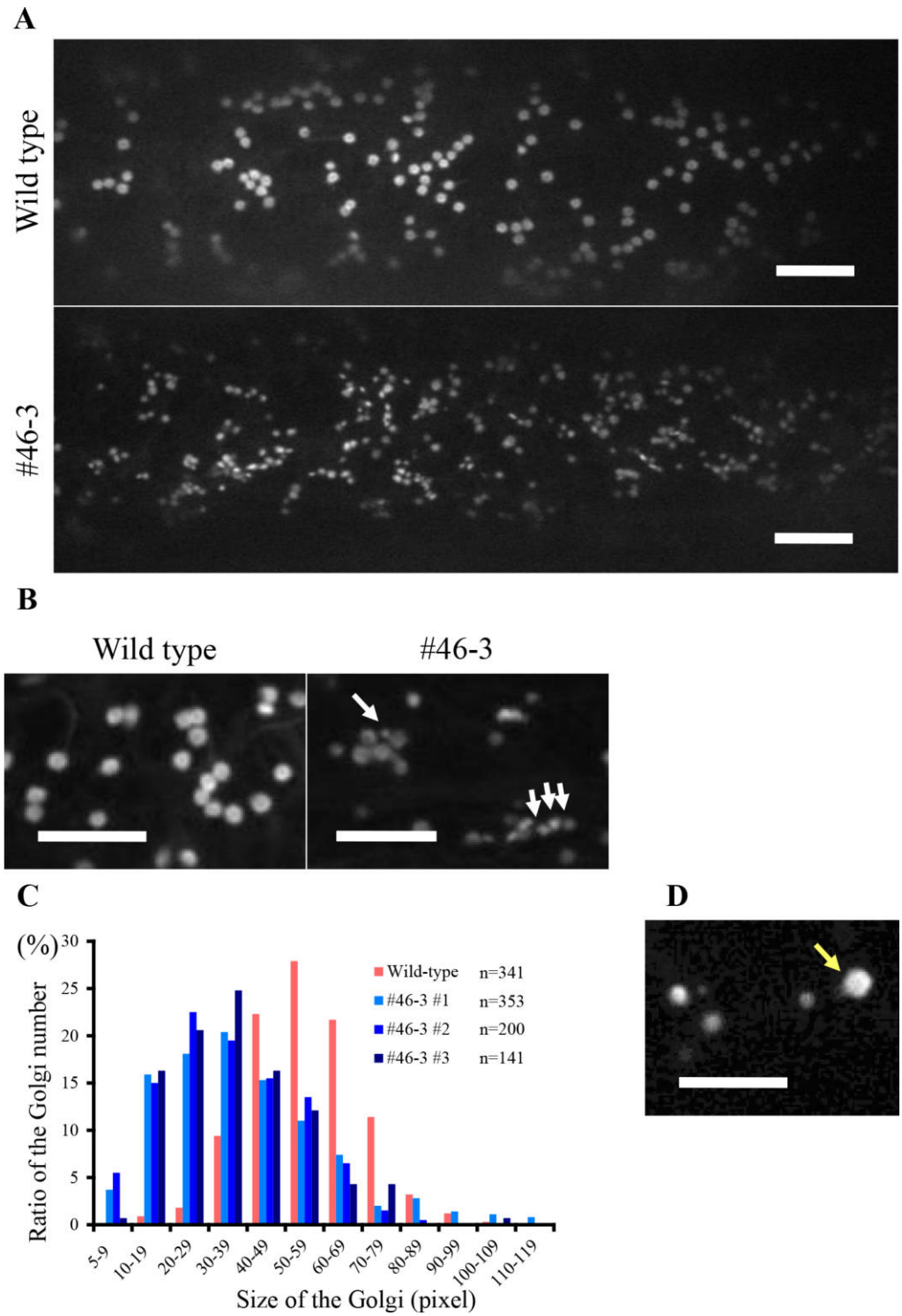

Fig. 1. #46-3 shows an abnormal Golgi morphology. (A) Confocal optical sections of leaf epidermal cells of third-leaf-petioles from the wild-type and the #46-3 mutant *A. thaliana* cells. Scale bar, 5 μm. (B) Close-up images of the wild-type and #46-3 mutant cells. White arrows indicate small Golgi structures in the #46-3 mutant. Scale bar, 5 μm. (C) Comparison of the Golgi size between the wild type and independent three lines of the #46-3 mutant. The Golgi sizes in 10 petiole cells were measured with ImageJ software and expressed as pixels. (D) Abnormally large Golgi in the #46-3 mutant. The size of the Golgi indicated by the yellow arrow is 119 pixels. Scale bar, 5 μm.

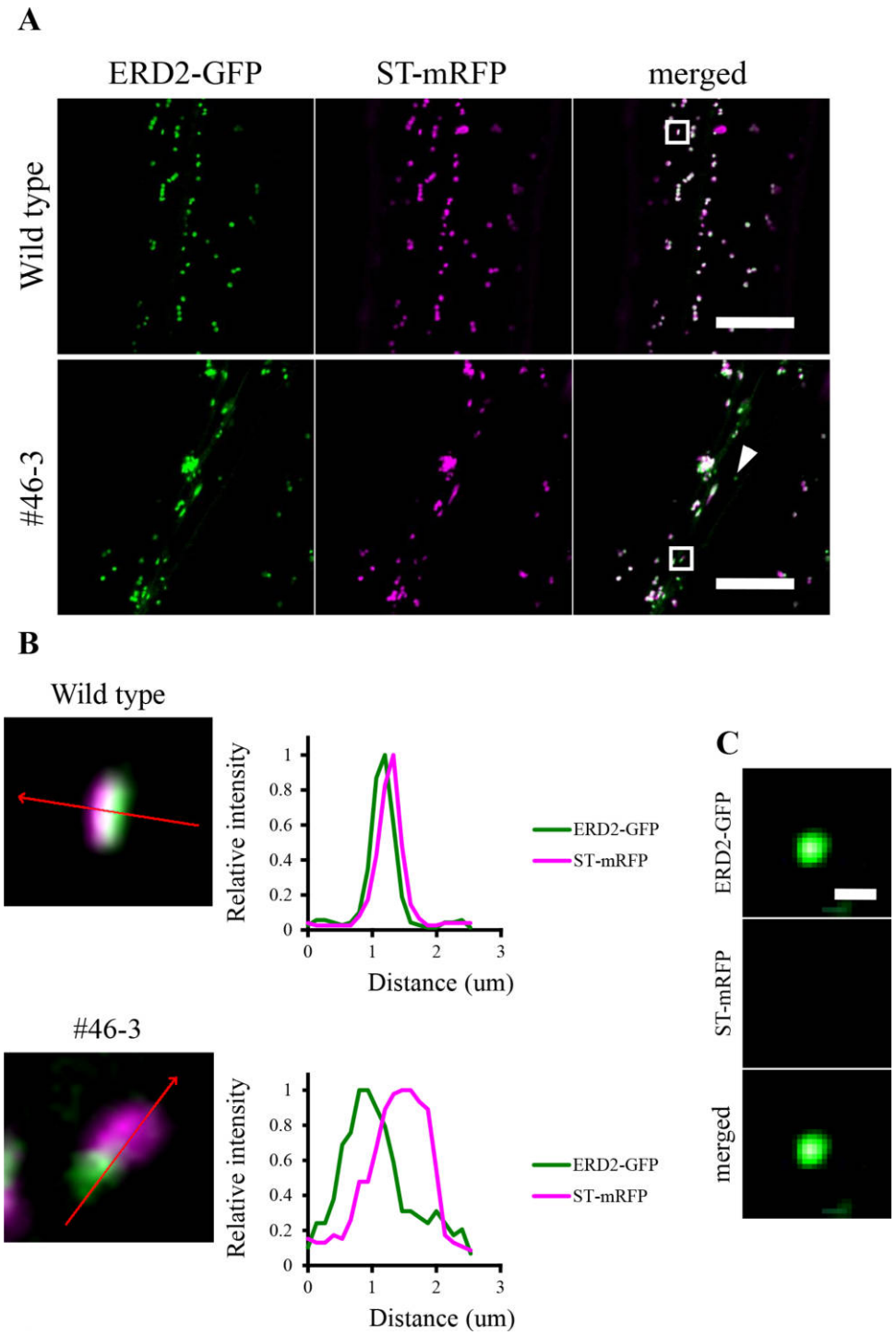

Fig. 2. Localization analysis of the *cis*-Golgi marker ERD2-GFP and the *trans*-Golgi marker ST-mRFP. (A) Two confocal slices of epidermal cells of third-leaf-petioles of the wild type and the #46-3 mutant. Scale bar, 10 μm. (B) The fluorescence profiles along the red arrows across the Golgi stacks indicated by boxes in (A). The intensity is shown relative to the maximum intensity in each signal of fluorescence, which is represented as 1. (C) A magnified view of the Golgi stack indicated by the arrowhead in (A). Note the lack of the ST-mRFP signal.

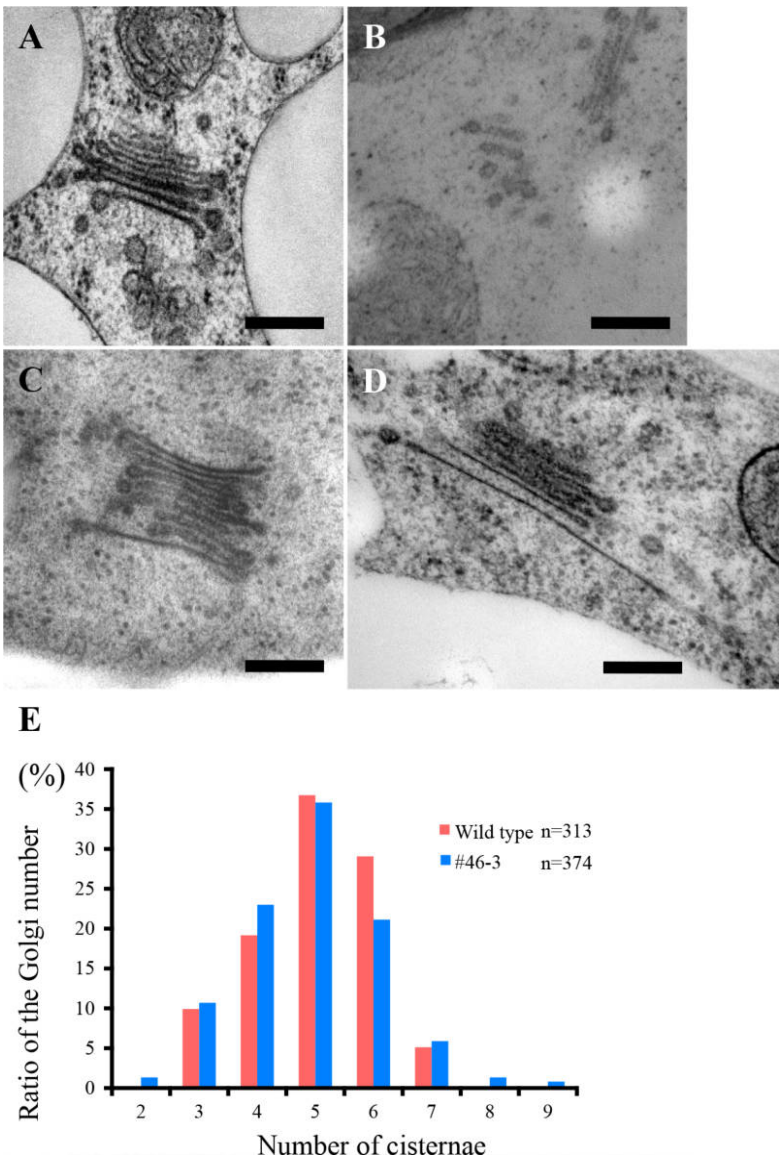

Fig. 3. Ultrastructure of the abnormal Golgi morphology. (A) An electron micrograph of the Golgi in the wild type. The cisternal number is 5 in this example. (B–D) Electron micrographs of the Golgi in the #46-3 mutant. In (B), the structures did not look like typical Golgi stacks but appeared to have smaller number (2–3) of cisternae. In contrast, the cisternal number of the Golgi is increased in (C) and the Golgi stack bears an extremely large *trans*-most Golgi cisterna in (D). Scale bar, 200 nm. (E) Histograms showing the cisternal number distribution in individual Golgi stacks.

wild type and #46-3 is shown as histograms in Fig. 3E. The cisternal numbers did not appear significantly different in the Golgi stacks between the wild type and the #46-3 mutant, the latter showing a broader distribution. As mentioned above, abnormal Golgi that did not show typical stacks might be overseen in electron micrographs. Combined with the fluorescence observation, we concluded that the #46-3 mutant had a pleiotropic defect in normal arrangement of Golgi stacks in both size and shape.

The #46-3 Golgi phenotype is linked to a mutation in the At4g04910 locus

To identify the mutation in the genome that caused the phenotype of #46-3, we proceeded to identify the mutation locus. We crossed the #46-3 plants with the wild-type plants (Col-0) expressing ERD2-GFP to determine the inheritance pattern. Segregation of the F2 population from the third backcross indicated that the #46-3 mutation was recessive to the wild type. To generate a mapping population, we crossed #46-3 with a different ecotype Landsberg

Fig. 4. Alignment of the amino acid sequences of NSF. Sequence alignment of a part of the D1 domain of NSF among different eukaryotic species is shown. Note that the sequence around the position D374 of Arabidopsis (colored) is highly conserved.

erecta. The genomic DNA of F2 plants exhibiting the abnormal phenotype was roughly mapped with simple sequence length polymorphism and cleaved amplified polymorphic sequence markers. Then, the candidate region containing the mutation was analyzed by the linkage analysis using a next-generation DNA sequencer. The results of these analyses nailed down the causal mutation on the upper arm of the chromosome 4 at 1–5.5 Mbp interval. Among nucleotide differences within this region, only 3 were predicted to be non-silent in open-reading frames. They were in the loci At4g02410, At4g02750, and At4g04910, which were annotated to encode L-type lectin-like protein kinase 1 (AtLPK1), tetratricopeptide repeat (TPR)-like superfamily protein, and *N*-ethylmaleimide-sensitive factor (NSF), respectively. Among these three, At4g04910 was of particular interest to us, because NSF is well known as a key protein required for membrane fusion. The At4g04910 locus of #46-3 had a G-to-A point mutation at the nucleotide number 2492290, which led to a GAT to AAT codon change resulting in the amino acid change from aspartic acid to asparagine at the residue position 374 (D374N). *A. thaliana* has only one ortholog of NSF in the genome. Comparison of NSF sequences indicates that this aspartate residue is very well conserved in eukaryotes (Fig. 4).

The missense mutation in NSF is responsible for the Golgi phenotype of #46-3

To examine whether the D374 mutation in NSF was indeed responsible for the observed phenotype, we performed a complementation test. We cloned the genomic DNA fragment from the wild-type plants containing the whole At4g04910 locus including the promoter and the open-reading frame and introduced into the #46-3 mutant. We analyzed the Golgi morphology in leaf petioles of two independent T2 seedlings under a confocal microscope. As shown in Fig. 5, the #46-3 phenotype in the Golgi shape (Fig. 5A) and the Golgi size distribution (Fig. 5B) was almost fully complemented. DNA fragments containing At4g02410 or At4g02750 did not complement the defect.

We also conducted an allelism test. We obtained from the ABRC stock center three *A. thaliana* lines containing T-DNA insertions at the *NSF* gene locus in the Col-0 background. We confirmed that T-DNA was inserted in the 5' UTR both in SALK_091598/SALK_138721 (at nucleotide 2495839) and in SAIL_1155_C06 (at nucleotide 2495824) and in the third exon in SAIL_620_E12 (at nucleotide 2495008) of the *NSF* gene. We could make a homozygous line of SALK_091598/SALK_138721 but not for SAIL_1155_C06 and SAIL_620_E12, probably because the complete knockout of NSF is lethal. Then, we crossed #46-3 with SAIL_1155_C06 to establish a heterozygous line and examined its Golgi morphology. As shown in Fig. 6, the Golgi phenotype seen by ERD2-GFP signals in the transformed #46-3/SAIL_1155_C06 plant phenocopied that of the #46-3 mutant under a confocal microscope (Fig. 6A).

Taken together, we concluded that the D374 missense mutation in NSF caused the Golgi morphology phenotype of #46-3.

Discussion

Morphology of organelles is considered to reflect their functions. Stacking of cisternae in the Golgi apparatus is one of the most striking structural features, which has been attracting many cell biologists, and is believed very important for efficient processing and sorting of cargo molecules. However, the fact that the budding yeast *S. cerevisiae* does not have a stacked structure of the Golgi yet managing efficient cargo processing leaves the significance of stacking elusive. From a mechanistic point of view, how these stacked structures are formed and maintained is also intriguing. The roles of Golgi matrix proteins have been argued for animal cells, but most of these molecules are not conserved in plants, whose Golgi nevertheless shows beautiful stacked structures. We have recently revealed by super-resolution confocal live imaging microscopy (SCLIM) (Kurokawa *et al.*, 2013) that Golgi stacks in tobacco cells

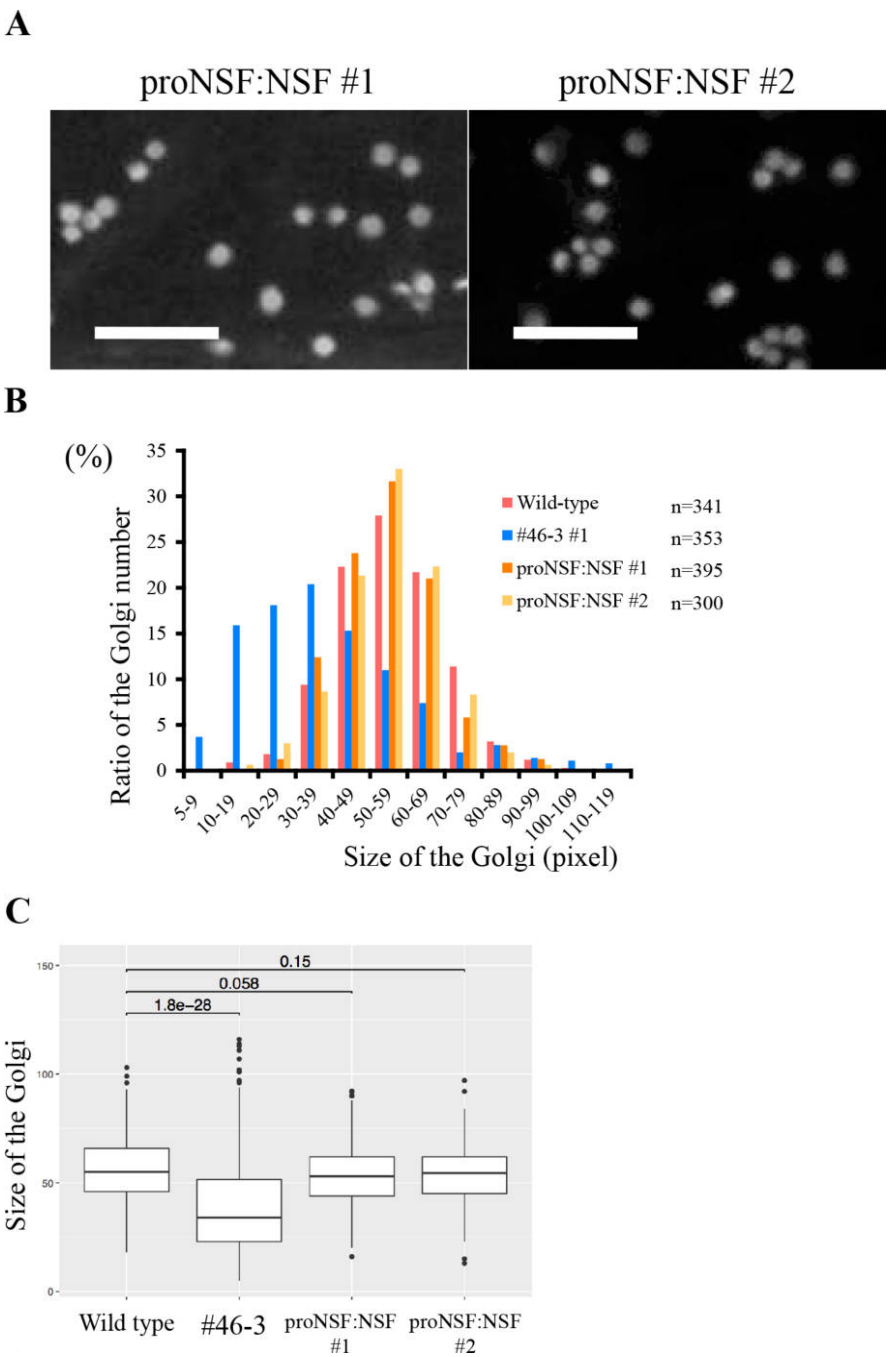

Fig. 5. The genomic DNA of *NSF* complements the phenotype of abnormal Golgi morphology in the #46-3 mutant. (A) Confocal optical sections of epidermal cells of third-leaf-petioles in two independent T2 seedlings, which express the whole sequence of *NSF* in the #46-3 background. Scale bar, 5 μm. (B) Histograms showing the Golgi size distribution. The Golgi size in 10 petiole cells were measured with ImageJ software. (C) Statistic analysis of the histograms in (B). The horizontal line in each box represents the median value of the distribution. The boundaries of a box represent the lower and upper quartile values. The whiskers extending vertically from the upper and lower portions of each box represent the extent of the rest of the data. Numbers denote *p* values based on Welch's test.

are formed in the order from *cis*- to *trans*-cisternae and that the presence of scaffold at *cis*-most side, which we named Golgi entry core compartment (GECCO), plays a role of receiving cargo from the ER (Ito *et al.*, 2012, 2017). Furthermore, computational simulation has implicated self-organizing properties of Golgi cisternae during reassembly

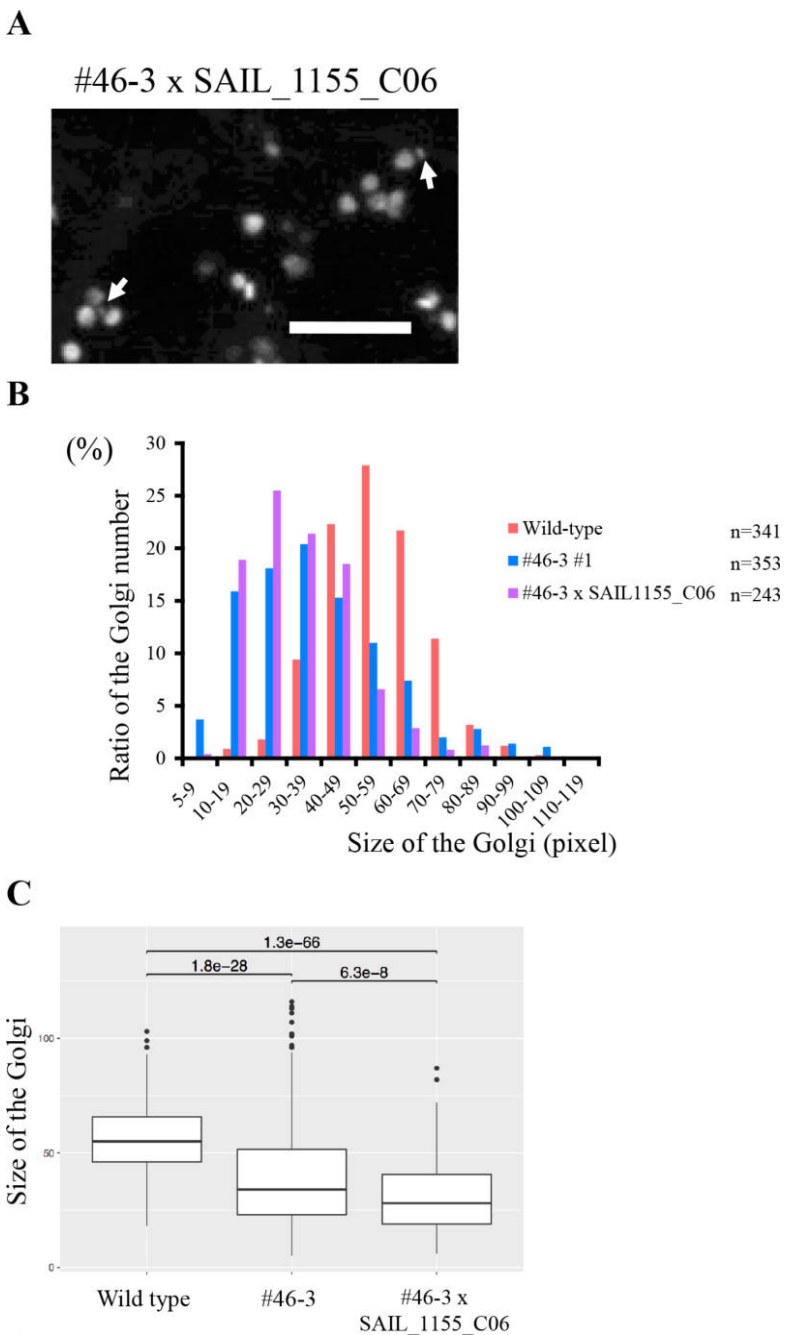

Fig. 6. The Golgi of the #46-3/SAIL_1155_C06 heterozygous line shows the abnormal phenotype. (A) Confocal optical sections of epidermal cells of third-leaf-petioles in the #46-3/SAIL_1155_C06 heterozygous seedlings. Arrows indicate small Golgi. Scale bar, 5 μm. (B) Histograms showing the Golgi size distribution. The Golgi size in 10 petiole cells were measured with ImageJ software. (C) Statistic analysis of the histograms in (B). The meanings of lines, boxes and whiskers are as in the legend of Fig. 5. Numbers denote *p* values based on Welch's test.

processes (Tachikawa and Mochizuki, 2017).

To obtain further insights into the molecular basis for Golgi morphogenesis in plant cells, we have sought for mutations that affect Golgi morphology in Arabidopsis by a forward-genetic approach. In the present paper, we have demonstrated that the mutant #46-3 has a D374N missense mutation in NSF, which is responsible for the morphological defect of the Golgi.

NSF is a key player in membrane fusion events

NSF, *N*-ethylmaleimide-sensitive factor, was first identified as a key protein functioning in intra-Golgi trafficking. Inactivation of the Golgi membrane by *N*-ethylmaleimide in a cell-free reconstitution system caused perturbation of intra-Golgi transport (Glick and Rothman, 1987). This assay allowed purification of NSF (Block *et al.*, 1988). As interacting molecules with NSF, SNAP was isolated (Weidman *et al.*, 1989), and as the membrane receptors for SNAP, SNARE proteins were discovered (Söllner *et al.*, 1993). All these components are now known to constitute the pivotal machinery for membrane fusion.

NSF is a member of the ATPases associated with diverse cellular activities plus (AAA+) family, which are present in all kingdoms of eukaryotes (Ryu *et al.*, 2016; Zhao and Brunger, 2016). The most important role of ATP hydrolysis by NSF is to disassemble the SNARE complex after membrane fusion. NSF is now known to be essential for numerous membrane fusion events (Südhof, 2013; Sutton *et al.*, 1998; Weber *et al.*, 1998).

As such, the NSF function is essential for many cellular activities and thus must be essential for life. Indeed, the *S. cerevisiae SEC18* gene that encodes NSF is essential for growth. Our results that *A. thaliana* lines that were homozygously null for NSF were never obtained from two T-DNA insertion lines (in this study), probably indicate that the complete loss of NSF is lethal.

The missense mutation of NSF that we identified as the cause of the abnormal Golgi morphology was D to N substitution at the amino acid residue #374. A D-to-N mutation is often regarded as subtle because the structural change in the side chain is small. It is probably why this mutant was obtained without an appreciable growth phenotype. Microscopically, the phenotype of this mutant is pleiotropic. At the fluorescence confocal microscope level, the Golgi size was in majority smaller than the wild type, but varies from very small ones, sometimes without clear association between *cis* and *trans* cisternae, to abnormally large ones, which were rather rare. At the ultrastructural level by transmission electron microscopy, abnormally small Golgi structures were hard to find, perhaps because they did not look like typical Golgi, but queer-shaped large Golgi stacks were occasionally observed.

Asp374 in the NSF-D1 domain is highly conserved among eukaryotes

In the process of membrane fusion, several reactions proceed in a sequential manner. The leading player is the SNARE proteins; R-SNARE on the vesicle membrane and the Qa-, Qb- and Qc-SNAREs on the target membrane, form 4-helix bundles to execute physical fusion of two lipid bilayers. After fusion, the SNARE bundles have to be disassembled for the next round of fusion reactions. NSF and SNAP play roles in this SNARE disassembly. Hydrolysis of ATP by NSF is essential for the disassembly reaction.

The molecular structure of NSF has been analyzed by X-ray crystallography (Lenzen *et al.*, 1998; May *et al.*, 1999). NSF consists of an amino-terminal region that interacts with other components of the vesicle trafficking machinery, followed by the two homologous ATP-binding cassettes, designated D1 and D2, which possess essential ATPase and hexamerization activities, respectively. The D374 residue of Arabidopsis NSF lies in the D1 domain near the ATP-binding site, around which the amino acid sequence is very well conserved among eukaryotes (Fig. 4). Thus the D374N mutation of Arabidopsis NSF may well affect its ATP-binding or hydrolysis activities of NSF, which should be examined in detail on purified proteins in the future.

Membrane fusion and the Golgi morphology

Now the question is how the lesion of NSF can affect the Golgi structure. Is it the membrane fusion events that are directly involved in cisternal arrangements? Regardless the model of cargo transport within the Golgi, it is obvious that the membranes in the Golgi have to be in a very dynamic equilibrium. Vesicle budding and membrane tubulation together with membrane fusion events must be always going on to maintain the steady-state morphology of the Golgi. Finding of a missense mutation in NSF, the essential factor of fusion, will provide us a clue to further our understanding of how the beautiful structure of the Golgi is formed and maintained.

Acknowledgments. We thank Emi Ito (International Christian University, Tokyo, Japan), Junpei Takagi (Konan University, Kobe, Japan) and Takashi Ueda (National Institute for Basic Biology, Okazaki, Japan) for valuable advice. This work was supported by a Grant-in-Aid for Scientific Research (S) (grant number 25221103) to A. N. from Japan Society for the Promotion of Science.

References

Bell, C.J. and Ecker, J.R. 1994. Assignment of 30 microsatellite loci to the linkage map of *Arabidopsis*. *Genomics*, **19**: 137–144.

Block, M.R., Glick, B.S., Wilcox, C.A., Wieland, F.T., and Rothman, J.E. 1988. Purification of an *N*-ethylmaleimide-sensitive protein catalyzing vesicular transport. *Proc. Natl. Acad. Sci. USA*, **85**: 7852–7856.

Boevink, P., Oparka, K., Santa, Cruz, S., Martin, B., Betteridge, A., and Hawes, C. 1998. Stacks on tracks: the plant Golgi apparatus traffics on an actin/ER network. *Plant J.*, **15**: 441–447.

Clough, S.J. and Bent, A.F. 1998. Floral dip: a simplified method for Agrobacterium-mediated transformation of *Arabidopsis thaliana*. *Plant J.*, **16**: 735–743.

Emr, S., Glick, B.S., Linstedt, A.D., Lippincott-Schwartz, J., Luini, A., Malhotra, V., Marsh, B.J., Nakano, A., Pfeffer, S.R., Rabouille, C., Rothman, J.E., Warren, G., and Wieland, F.T. 2009. Journeys through the Golgi—taking stock in a new era. *J. Cell Biol.*, **187**: 449–453.

Glick, B.S. and Rothman, J.E. 1987. Possible role for fatty acyl-coenzyme A in intracellular protein transport. *Nature*, **326**: 309–312.

Glick, B.S. and Nakano, A. 2009. Membrane traffic within the Golgi apparatus. *Annu. Rev. Cell Dev. Biol.*, **25**: 113–132.

Glick, B.S. and Luini, A. 2011. Models for Golgi traffic: a critical assessment. *Cold Spring Harbor Perspect. Biol.*, **3**: a005215.

Ishii, M., Suda, Y., Kurokawa, K., and Nakano, A. 2016. COPI is essential for Golgi cisternal maturation and dynamics. *J. Cell Sci.*, **129**: 3251–3261.

Ito, Y., Uemura, T., Shoda, K., Fujimoto, M., Ueda, T., and Nakano, A. 2012. *cis*-Golgi proteins accumulate near the ER exit sites and act as the scaffold for Golgi regeneration after brefeldin A treatment in tobacco BY-2 cells. *Mol. Biol. Cell*, **23**: 3203–3214.

Ito, Y., Uemura, T., and Nakano, A. 2017. Golgi entry core compartment functions as the COPII-independent scaffold for ER-Golgi transport in plant cells. *J. Cell Sci.*, in press.

Karimi, M., Inzé, D., and Depicker, A. 2002. GATEWAY vectors for Agrobacterium-mediated plant transformation. *Trends Plant Sci.*, **7**: 193–195.

Konieczny, A. and Ausubel, F.M. 1993. A procedure for mapping *Arabidopsis* mutations using co-dominant ecotype-specific PCR-based markers. *Plant J.*, **4**: 403–410.

Kurokawa, K., Ishii, M., Suda, Y., Ichihara, A., and Nakano, A. 2013. Live cell visualization of Golgi membrane dynamics by super-resolution confocal live imaging microscopy. *Methods Cell Biol.*, **118**: 235–242.

Lenzen, C.U., Steinmann, D., Whiteheart, S.W., and Weis, W.I. 1998. Crystal structure of the hexamerization domain of N-ethylmaleimide-sensitive fusion protein. *Cell*, **94**: 525–536.

Losev, E., Reinke, C.A., Jellen, J., Strongin, D.E., Bevis, B.J., and Glick, B.S. 2006. Golgi maturation visualized in living yeast. *Nature*, **441**: 1002–1006.

Matsuura-Tokita, K., Takeuchi, M., Ichihara, A., Mikuriya, K., and Nakano, A. 2006. Live imaging of yeast Golgi cisternal maturation. *Nature*, **441**: 1007–1010.

May, A.P., Misura, K.M., Whiteheart, S.W., and Weis, W.I. 1999. Crystal structure of the amino-terminal domain of *N*-ethylmaleimide-sensitive fusion protein. *Nat. Cell. Biol.*, **1**: 175–182.

Mollenhauer, H.H. and Morré, D.J. 1991. Perspectives on Golgi apparatus form and function. *J. Electron Microsc. Tech.*, **17**: 2–14.

Nilsson, T., Au, C.E., and Bergeron, J.J. 2009. Sorting out glycosylation enzymes in the Golgi apparatus. *FEBS Lett.*, **583**: 3764–3769.

Noguchi, T. 1978. Transformation of the Golgi apparatus in the cell cycle, especially at the resting and earliest developmental stages of a green alga, *Micrasterias Americana*. *Protoplasma*, **95**: 73–88.

Papanikou, E., Day, K.J., Austin, J., and Glick, B.S. 2015. COPI selectively drives maturation of the early Golgi. *eLife*, **4**: e13232.

Preuss, D., Mulholland, J., Franzusoff, A., Segev, N., and Botstein, D. 1992. Characterization of the *Saccharomyces* Golgi complex through the cell cycle by immunoelectron microscopy. *Mol. Biol. Cell*, **3**: 789–803.

Rothman, J.E. and Wieland, F.T. 1996. Protein sorting by transport vesicles. *Science*, **272**: 227–234.

Ryu, J.K., Jahn, R., and Yoon, T.Y. 2016. Review: Progresses in understanding N-ethylmaleimide sensitive factor (NSF) mediated disassembly of SNARE complexes. *Biopolymers*, **105**: 518–531.

Söllner, T., Bennett, M.K., Whiteheart, S.W., Scheller, R.H., and Rothman, J.E. 1993. A protein assembly-disassembly pathway in vitro that may correspond to sequential steps of synaptic vesicle docking, activation, and fusion. *Cell*, **75**: 409–418.

Staehelin, L.A. and Kang, B.H. 2008. Nanoscale architecture of endoplasmic reticulum export sites and of Golgi membranes as determined by electron tomography. *Plant Physiol.*, **147**: 1454–1468.

Südhof, T.C. 2013. Neurotransmitter release: the last millisecond in the life of a synaptic vesicle. *Neuron*, **80**: 675–690.

Sutton, R.B., Fasshauer, D., Jahn, R., and Brunger, A.T. 1998. Crystal structure of a SNARE complex involved in synaptic exocytosis at 2.4 A resolution. *Nature*, **395**: 347–353.

Tachikawa, M. and Mochizuki, A. 2017. Golgi apparatus self-organizes into the characteristic shape via postmitotic reassembly dynamics. *Proc. Natl. Acad. Sci. USA*, **114**: 5177–5182.

Takeuchi, M., Ueda, T., Sato, K., Abe, H., Nagata, T., and Nakano, A. 2000. A dominant negative mutant of Sar1 GTPase inhibits protein transport from the endoplasmic reticulum to the Golgi apparatus in tobacco and *Arabidopsis* cultured cells. *Plant J.*, **23**: 517–525.

Takeuchi, M., Ueda, T., Yahara, N., and Nakano, A. 2002. Arf1 GTPase plays roles in the protein traffic between the endoplasmic reticulum and the Golgi apparatus in tobacco and *Arabidopsis* cultured cells. *Plant J.*, **31**: 499–515.

Uchida, N., Sakamoto, T., Kurata, T., and Tasaka, M. 2011. Identification of EMS-induced causal mutations in a non-reference *Arabidopsis thaliana* accession by whole genome sequencing. *Plant Cell Physiol.*, **52**: 716–722.

Weber, T., Zemelman, B.V., McNew, J.A., Westermann, B., Gmachl, M., Parlati, F., Söllner, T.H., and Rothman, J.E. 1998. SNAREpins: minimal machinery for membrane fusion. *Cell*, **92**: 759–772.

Weidman, P.J., Melançon, P., Block, M.R., and Rothman, J.E. 1989. Binding of an *N*-ethylmaleimide-sensitive fusion protein to Golgi membranes requires both a soluble protein(s) and an integral membrane receptor. *J. Cell Biol.*, **108**: 1589–1596.

Zhao, M. and Brunger, A.T. 2016. Recent Advances in Deciphering the Structure and Molecular Mechanism of the AAA+ ATPase *N*-Ethylmaleimide-Sensitive Factor (NSF). *J. Mol. Biol.*, **428**: 1912–1926.

(Received for publication, December 13, 2017, accepted, January 29, 2018 and published online, February 2, 2018)